Available online at www.sciencedirect.com
ScienceDirect
Journal of Power Sources 178 (2008) 610–619
JOURNAL OF POWER SOURCES
www.elsevier.com/locate/jpowsour

Surface chemistry and physical properties of Nafion/polypyrrole/Pt composite membrane prepared by chemical in situ polymerization for DMFC

HoSeok Park [a], YoJin Kim [a], Yeong Suk Choi [b], Won Hi Hong [a,*], Doohwan Jung [c]

[a] *Department of Chemical and Biomolecular Engineering (BK21 Program), KAIST, 373-1 Guseong-dong, Yuseong-gu, Daejeon, Republic of Korea*
[b] *Energy & Environment Laboratory, Samsung Advanced Institute of Technology (SAIT), P.O. Box 111, Suwon, Republic of Korea*
[c] *Advanced Fuel Cell Research Center, Korea Institute of Energy Research, 71-2 Jang-dong, Yuseong-gu, Daejeon, Republic of Korea*

Received 8 July 2007; received in revised form 21 August 2007; accepted 21 August 2007
Available online 25 August 2007

Abstract

We modified Nafion by means of chemical in situ polymerization of pyrrole monomers with platinum (Pt) precursors for an application into an electrolyte of direct methanol fuel cells (DMFCs). SEM and EPMA exhibited the presences of polypyrrole and Pt at the surface region of Nafion, after diffusing and polymerizing pyrrole monomers with Pt precursors. XPS and FT-IR spectra were used to characterize the surface of Naf–Ppy–Pt composite membranes, demonstrating that pyrrolinum groups of polypyrrole were interacted with sulfonic groups or Pt precursors ($PtCl_6^-$ or $PtCl_4^-$). After in situ polymerization of pyrrole monomers, the morphological reorganization of sulfonic groups in Naf–Ppy–Pt composite membranes occurred via electrostatic interaction. Thermal stability, proton conductivity, methanol permeability, and cell performance of composite membranes were analyzed by TGA, AC impedance, refractometer, and potentiostat. Naf–Ppy–Pt composite membranes had higher thermal stabilities of sulfonic groups and side chains than Nafion and Naf–Ppy as a result of the interaction between Nafion–$SO_3^-\cdots$polypyrrole–NH_2^+ and the presence of thermally stable Pt. The cell performance of Naf–Ppy–Pt 0 0 2 was enhanced significantly compared to that of Nafion under the specific condition, due to more reduction of methanol crossover than that of proton conductivity. Therefore, this synthetic method offers a facile way to improve physical properties of polymer electrolyte for the fabrication of advanced composite membranes.

Keywords: Composite membrane; Electrolyte; Nafion; Polypyrrole; Pt; DMFC

1. Introduction

In recent years, much attention has been focused on DMFCs as an attractive energy generating system in the field of small and portable electrochemical or electronic devices such as cellular phones and laptop computers. Although DMFC has advantages over hydrogen-based fuel cells in terms of fuel handling and simple design owing to the use of methanol as safe fuel, there is a severe problem that the methanol crossover from anode through membrane to cathode by electro-osmotic drag and diffusion decreases the overall performance of the cell due to fuel loss and mixed potential [1–3]. Polymer electrolyte membranes (PEMs) become an important part of DMFC as well as other fuel cells, in view of not only playing a role of conducting protons but also becoming a key component to solve methanol crossover. Among them, Nafion, which is a commercially representative perfluorosulfonate ionomer, is used as a proton conductor with reasonable chemical and thermal stability [4,5]. Nafion is an ionomer consisting of hydrophobic backbone and hydrophilic side chain with sulfonic groups [4,5]. Phase separation occurs between hydrophobic and hydrophilic regions in a hydrated state, resulting in the construction of ionic clusters. Although Nafion obtains desirable physical properties such as thermal and mechanical stabilities owing to its pristine structure for an application of DMFC membrane, it is very difficult to reduce the methanol crossover with

* Corresponding author. Tel.: +82 42 869 3919.
E-mail addresses: milleniumphs@kaist.ac.kr (H. Park), Ester@kaist.ac.kr (Y. Kim), yeongsuk.choi@samsung.com (Y.S. Choi), whhong@kaist.ac.kr (W.H. Hong), doohwan@kier.re.kr (D. Jung).

0378-7753/$ – see front matter © 2007 Elsevier B.V. All rights reserved.
doi:10.1016/j.jpowsour.2007.08.050

maintaining considerable proton conductivity, because ionic clusters are the transport pathway of methanol as well as proton [4–6].

To overcome above trade-offs for DMFC, many strategies have been investigated to improve cell performance by controlling two kinds of transport properties. Amongst them, Nafion/conducting polymer composites have been extensively studied to apply into electrodialysis and sensor as well as PEMs due to their unique properties [7]. For example, they can decrease methanol crossover effectively by means of combining the high cationic conductivity of the perfluorosulfonic ionomer with the electrocatalytic activity of the conducting polymer or using conducting polymer as fillers for a barrier effect on methanol transfer [8,9]. In this research, we focused on Nafion/polypyrrole composites among various Nafion/conducting polymer systems. Pickup and his coworkers demonstrated the chemical in situ polymerization mechanism of pyrrole in the Nafion matrix and the enhancement of the performance in DMFC [7,8]. We reported that the nano-sized polypyrrole particles were mainly present near the surface rather than the internal space by controlling the concentration and diffusion time of pyrrole monomers [9]. In addition, some researches demonstrated that pyrrole monomers were diffused into and in situ polymerized at only one side of membrane by using diffusion method, thereby controlling the location of thin layer among two faces of Nafion matrix [10,11]. In the case of electrochemical synthesis compared to chemically oxidative polymerization, the rate, extent, and location of polymerization could be controlled by electrochemical conditions such as voltage or current as well as polymerization time and monomer concentration [12–14].

Much work has been devoted on fabricating the composite of conducting polymer and metal nanoparticles as a novel electrode material or sensor owing to its high electrocatalytic activity or electrochemical property [15–17]. Lee et al. reported that a novel method of deposing thin Pt catalysts on Nafion membranes impregnated with polypyrrole was proposed for unitized regenerative fuel cells (URFCs) [18]. However, few studies have been undertaken on the application of a perfluorosulfonic ionomer/conducting polymer/metal composite system into an electrolyte of fuel cells. Herein, we report the synthesis of Nafion/polypyrrole/Pt composite membranes and characterization of their surface and physical properties for an application into an electrolyte. The physical and transport properties of Nafion/polypyrrole/Pt composite membranes were compared with those of Nafion/polypyrrole composite membrane, which were optimized by previous our results [9].

2. Experimental

2.1. Materials

Nafion 115 membrane, which was supplied by E.I. Dupont de Nemours & Co., had an equivalent weight of 1100 g for each sulfonic acid. Pyrrole monomer was purchased from Sigma–Aldrich and purified by distillation to remove impurities, oligomers, and polymerization retarders. Extra-pure hydrogen peroxide (H_2O_2, 35 wt%) was purchased from Junsei chemical and used as an oxidant for polymerization. H_2PtCl_6 was chosen as a Pt precursor and $NaBH_4$ as a reductant, which were supplied by Junsei chemical.

2.2. Preparation of the composite membrane

Nafion membranes were prepared as follows [9]. Before Nafion membranes were modified, they were purified by first heating them in deionized water containing 3 wt% H_2O_2 for 1 h at about 70–80 °C, and then repeated the process four times in deionized water to completely remove all traces of H_2O_2. A similar pretreatment was performed in 1 M H_2SO_4 for 1 h, and then repeated the treatment three times in deionized water to remove the sulfuric acid completely. The pretreated Nafion membranes were dried at room temperature (25 °C) under vacuum for 24 h. Pyrrole monomers were dispersed in deionized water and controlled to the specific concentration at 0.1 M. The Pt precursors were mixed with an aqueous pyrrole solution, dispersed by sonification, and controlled to the wanted concentration ranged from 10^{-4} to 2×10^{-2} M.

The prepared Nafion membranes were immersed for 5 min in an aqueous pyrrole monomer and Pt precursor solution. To in situ polymerize the pyrrole monomers in an aqueous solution via oxidative polymerization by an oxidant, they were immersed in 30 wt% H_2O_2 for 5 min at room temperature. After the in situ polymerization, Pt precursors were reduced by 2 M $NaBH_4$ and washed by deionized water for 1 h at 80 °C, respectively. The modified membranes were post-treated by 2 M methanol and washed by deionized water for 1 h at 80 °C, respectively, in order to remove the unreacted pyrrole monomers, impurities, and excess reductants. All samples were treated with nitric acid and sulfuric acid to change all the composite membranes into an H form. In order to prevent oxidative degradation of polypyrrole from acidic components, nitric and sulfuric acid were diluted into 1 M and acid-treatment was performed for 1 h at 80 °C, respectively. After nitric and sulfuric acid-treatment, no color changes attributed to the extraction of polpyrroles or Pt precursors were observed in nitric and sulfuric acid solution. Each acid-treatment was followed by washing step with deionized water. The obtained composite membranes are notated as Naf–Ppy–Pt 0 0 1 at 10^{-4} M, Naf–Ppy–Pt 0 0 2 at 5×10^{-3} M, Naf–Ppy–Pt 0 0 3 at 10^{-2} M and Naf–Ppy–Pt 0 0 4 at 2×10^{-2} M Pt precursor with 0.1 M pyrrole monomers, and Naf–Ppy at only 0.1 M pyrrole monomers.

The procedures to prepare the dried or rehydrated samples before any characterization step are as follows. All samples were dried under vacuum at room temperature for 1 week. The dried samples in the drying state were carefully sealed to prevent additional water absorption before any measurement. To prepare the rehydrated samples, the pre-dried samples were immersed in deionized water for 1 week and kept in the sealed Petri dish full of the deionized water. As soon as taking out the sample from the deionized water, all measurements were immediately carried out to maintain the levels of hydration.

2.3. Characterization

SEM images were obtained by a Field Emission Scanning Electron Microscope (Philips SEM 535M, installed at Korea Basic Science Institute) equipped with schottky based field emission gun. After immersing in liquid N_2, membranes were fractured as soon as taking out them in order to obtain images of cross-section.

The Pt profiles of the composite membranes were observed through an Electron Probe Micro Analyzer (EPMA, SX-50, Cameca). The measurement was carried out at 15 kV, 20 nA and 3000 ms per point.

Elemental analysis was performed within the accuracy of 0.3% by elemental analyzer, which is EA1110-FISONS, manufactured by ThermoQuest Italia SPA (CE Instruments). C, H, O, N and S elements of membrane were analyzed in the range of 0.01–100%. Total weight percent of the incorporated polypyrrole was calculated from the weight percent of nitrogen. Total weight percent of all fillers was calculated by measuring the weights of dried membranes before and after polymerization. The weight percent of Pt was calculated by subtracting weight percent of polypyrrole from total weight percent of all fillers.

FT-IR ATR spectra were collected on a JASCO FT-IR 470 plus as attenuated total reflection to measure dense polymer film. Each spectrum, which was recorded as the average of 12 scans with a resolution of 4 cm^{-1}, was collected from 4000 to 650 cm^{-1}. The pressure was equal in all samples to avoid differences caused by the pressure and penetrating depth.

XPS was used to analyze the changes in the chemical environment in the process of modification of Nafion by means of in situ polymerization. VG electron spectroscopy for chemical analysis (ESCA) 2000 was used at high vacuum (10^{-10} Torr), equipped with monochrometer (quartz), twin X-ray source (Mg/Al target) and hemispherical analyzer. To compensate for charging effects, binding energies were corrected for covalent C 1s at 284.6 eV after curve fitting. After a background correction, curve fitting were carried out by using mixed Gaussian–Lorentzian function.

To analyze the thermal stability of each sample, thermogravimetric analysis (TGA) was carried out using a Dupont 2200 thermal analysis station. After drying each sample, it is heated from 30 to 800 °C at the rate of 20 °C min^{-1} under a nitrogen atmosphere.

The proton conductivity of membranes at room temperature was measured by the AC impedance spectroscopy over a frequency range of 10^{-1} to 10^{6} Hz with 10 mV. A system based on a Solatron 1255 Frequency Response Analyzer, was used to measure the proton conductivities of membranes in a fully hydrated state along the cross-sectional direction with a two-point probe cell, as described before [19,20]. The conductivity of the sample was obtained by using a Nyquist plot from complex impedance analysis. The real and imaginary parts of the complex impedance were plotted and the proton conductivity was obtained from the bulk resistance found in complex impedance diagram. The proton conductivity can be calculated by using this equation $\sigma = L/RA$, where L and A are the thickness of the sample and the surface area of the electrode, and R is the resistance of membrane from the impedance data. Relative proton conductivities of composite membranes were obtained by dividing the measured values by that of pristine Nafion.

Methanol permeability was measured by means of a device described by previous literatures [19,20]. The diffusion cell consisting of two compartments, was separated by vertical membrane. One compartment of the cell was filled with deionized water. The other compartment was filled with a mixture solution of methanol and deionized water (5/5, v/v). The compartments were stirred continuously during permeability measurement. A refractometer (ATAGO 3T) was used to measure the concentration of the methanol. Relative methanol permeabilities of composite membranes were obtained by dividing by that of pristine Nafion.

Cell performance was evaluated by using a DMFC unit cell and measured with a potentiostat (263A Power Booster) which recorded the cell potential from the circuit voltage under constant current conditions. Carbon papers (TORAY) were wet-proofed and coated with gas diffusion layers and subsequent electrocatalyst layers. Membrane electrode assembly (MEA) was manufactured as follows this literature [9]. The cathode electrode with Pt (unsupported Pt Black, Johnson–Matthey Inc.) loading of 2 mg cm^{-2} and the anode one with Pt/Ru (unsupported Pt/Ru 50/50 (atom/atom) black, Johnson–Matthey Inc.) loading of 2 mg cm^{-2} were prepared by blushing method. Its active area was 2 cm × 2 cm. All electrodes were impregnated with Nafion^{TM} ionomer solution (Sigma–Aldrich). Two electrodes and polymer membrane were hot-pressed at 120 °C and 100 kgf cm^{-2} for 2 min. The performances of all samples were evaluated at room temperature under atmospheric conditions. Methanol solution of 3 or 6 M was supplied to the anode side of the single cell at the rate of 3 cm^3 min^{-1}, whereas oxygen gas was supplied to the cathode side of the single cell at the rate of 300 cm^3 min^{-1}. Measurement range of current was from 0 to 1 A.

3. Results and discussion

3.1. Synthesis of Nafion/polypyrrole/Pt composite membrane

Recently, we reported that when the nano-sized polypyrrole or palladium particles were dominantly present at the surface region, cell performance was improved by reducing effectively methanol crossover [9,21]. In particular, the optimized cell performance of Naf–Ppy composite membranes was obtained from the preferential existence of polypyrrole at the surface owing to the effective reduction of methanol crossover, as polypyrrole nanoparticles at internal space played a role of resisting proton conduction as well as methanol crossover [9]. When palladium nanoparticles were also present at the surface region, the modified membrane obtained the enhanced cell performance by means of tortuous pathway for methanol crossover and low interfacial resistance between electrolyte and catalyst layer [21]. In addition to above examples, there are some instances to explain the relationship between surface chemistry of nanocomposite and favorable effect of functional materials existing at the surface of matrix on the physical and transport properties

[21–24]. The characterization of the surface on the modified membrane is of prime importance in terms of the enhancement of performance by incorporating functional materials into the surface region of matrix for an applicative point of view as well as the investigation into surface chemistry of polymer based-composite materials for a scientific point of view. As a result of that, we chose the concentration of pyrrole monomers at 0.1 M, where polypyrrole was mainly present at

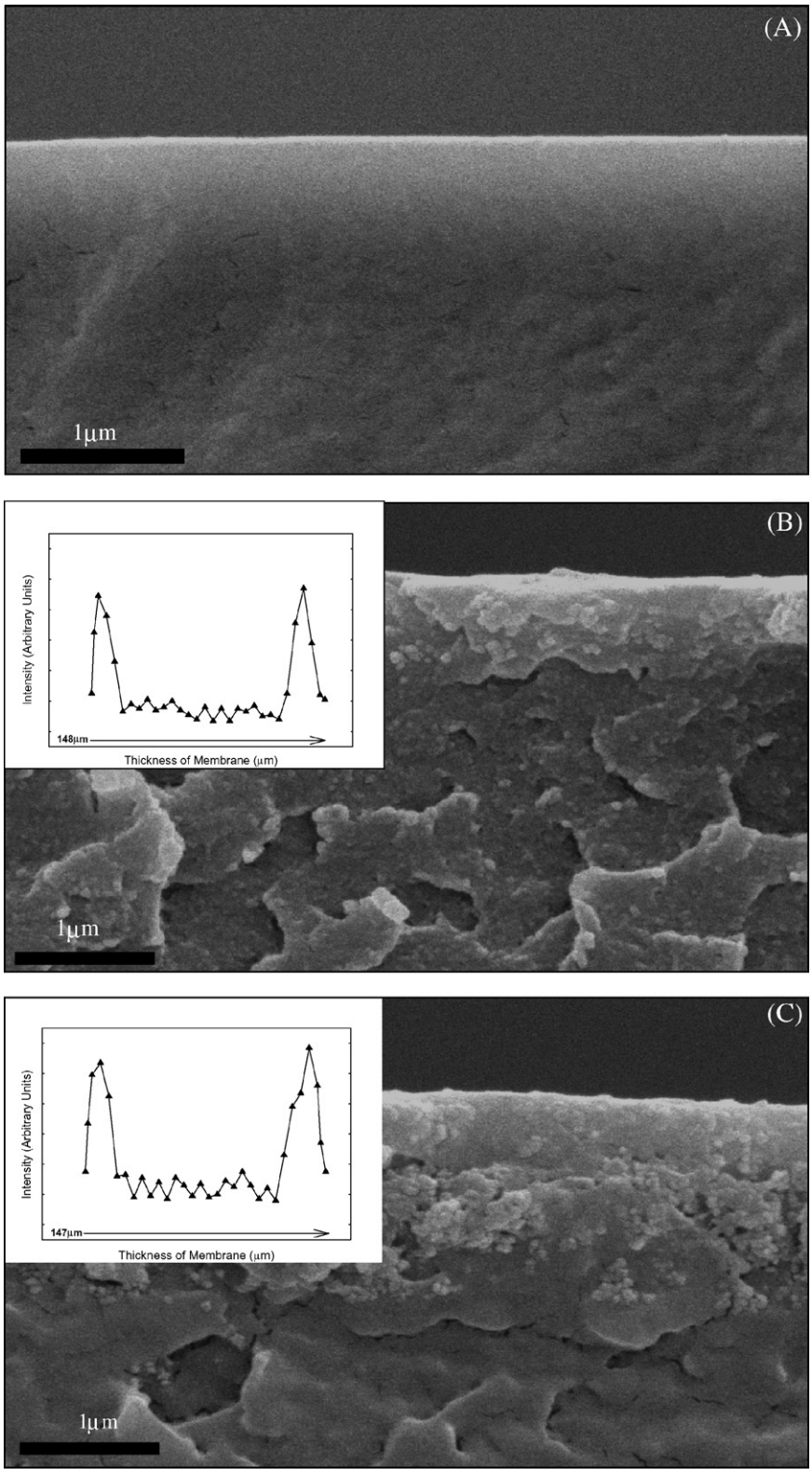

Fig. 1. SEM images of cross-section of (A) Nafion, (B) Naf–Ppy–Pt 0 0 2, and (C) Naf–Ppy–Pt 0 0 4 composite membranes. Insets are Pt profile along cross-section of composite membranes by EPMA.

the surface rather than bulk as reported by our previous results [9].

Fig. 1 presents SEM images of cross-section of Nafion, Naf–Ppy–Pt 0 0 2, and Naf–Ppy–Pt 0 0 4. In the case of pristine Nafion, smooth and dense structure was detected, whereas the composite membranes of Naf–Ppy–Pt 0 0 2 and 0 0 4 exhibited a rougher surface associated to the presence of polypyrrole and Pt. After chemical in situ polymerization of pyrrole monomers in the presence of Pt precursors, some of white aggregates and cracks were observed around the surface of composite membranes. These cracks were likely due to the occurrence of the fracture attributed to the increase in the brittleness of composite membrane in the process of preparing the cross-section of membrane for the measurement of SEM images, as polypyrrole and Pt were mainly distributed within the skin layer at the surface. In comparison to SEM image of Naf–Ppy composite membrane as reported by a previous literature [25], white spots around the surface were related to the dispersion of polypyrrole in the Nafion matrix. Unfortunately, polypyrrole and Pt were not distinguished from SEM images respectively, despite the differences of electron densities between polypyrrole and Pt. It may be that the size of Pt exceeded the detection range of SEM measurement. However, the existence of Pt particles around the surface of membrane was confirmed by EPMA profile, as shown in insets of Fig. 1(B) and (C). In addition to the morphological changes after in situ polymerization, the color of transparent Nafion was changed into dark brown. Fig. 2 shows the changes in the content of polypyrrole and Pt after chemical in situ polymerization. In this experimental range, despite the variation on the concentration of Pt precursors, the content of polypyrroles was hardly changed within the range of 0.2 wt%, while the content of Pt increased with the concentration of Pt precursors. Therefore, when pyrrole monomers with Pt precursors were incorporated into Nafion matrix by diffusion and polymerized at the surface, they could be existed at the surface region under the specific experimental condition. Although interactions between pyrrole monomers and Pt precursors during oxidative polymerization were not explained clearly, polypyrrole and Pt were mainly existed at the surface region. These results reveal requirements for characterizing the surface of composite membranes.

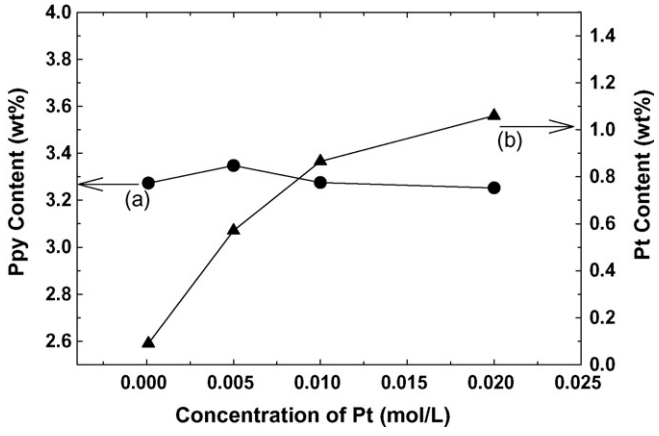

Fig. 2. Changes in the content of (a) polypyrrole and (b) Pt as a function of concentration of Pt precursor after chemical in situ polymerization.

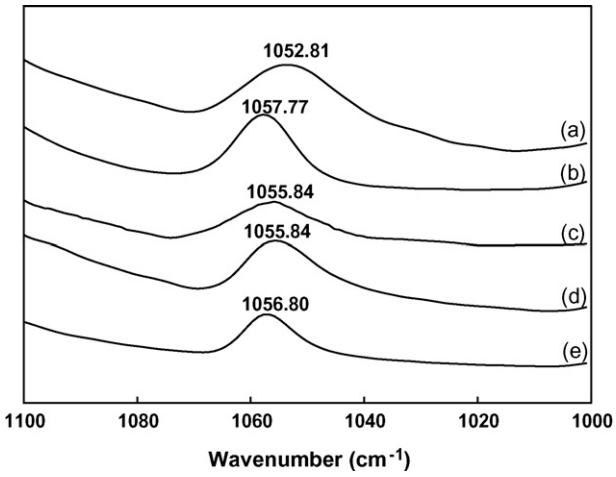

Fig. 3. FT-IR ATR spectra of 1100–1000 cm^{-1} region of (a) dried Nafion, (b) hydrated Nafion, (c) Naf–Ppy, (d) Naf–Ppy–Pt 0 0 2, and (e) Naf–Ppy–Pt 0 0 4.

3.2. Surface characterization of composite membrane

The changes in the chemical environment of surface were analyzed by FT-IR ATR and XPS, in order to investigate correlation between atoms or groups of components constituting composite membranes. It is needed to keep in mind that FT-IR ATR can detect chemical species found within few micrometers, whereas XPS can probe only depth of ca. 10 nm [24].

Fig. 3 shows the symmetric SO_3^- stretching vibration bands of dried Nafion, hydrated Nafion, dried Naf–Ppy, dried Naf–Ppy–Pt 0 0 2, and dried Naf–Ppy–Pt 0 0 4 around 1050 cm^{-1}. The shift of this peak was induced by the changes in polarization of the S–O dipole by means of the effect of chemical environment or surrounding [26]. When sulfonic groups of Nafion were interacted with cations or positively charged functional groups, the location of symmetric SO_3^- stretching band was changed. Furthermore, the degree of hydration affected significantly the peaks of sulfonate groups which are the dissociation forms of sulfonic groups [27]. Thus, the shift of SO_3^- peak in hydrated Nafion and dried composite membranes relative to dried Nafion, was associated with the changes in electrostatic interaction between sulfonic groups of Nafion and counterions of ionic surrounding. In a similar manner to Naf–Ppy system, positively charged pyrrolinum groups of polypyrrole were also interacted with sulfonic groups of Nafion in Naf–Pt–Ppy composite membrane, despite the simultaneous incorporation of pyrrole monomers and Pt precursor into Nafion matrix. As seen in Fig. 4(A), XPS analysis of N(1s) of Nafion, Naf–Ppy, Naf–Ppy–Pt 0 0 2 before reduction, and Naf–Ppy–Pt 0 0 2 after reduction was performed to confirm the interaction between pyrrolium groups of polypyrrole and sulfonic groups of Nafion clearly. The absence of N(1s) peaks in Nafion demonstrates that they are related to the state of nitrogen atoms in polypyrrole of composite membranes. There were four different N(1s) environments around the binding energies of 398, 400, 401 and 402 eV. The lowest binding energy corresponds to immine defects (typical N(1s) binding energies for immines are in the range of 397–399 eV) [28]. The binding energy around 400 eV is

assigned to freely neutral N–H from pyrrole repeating units [28]. Two peaks at around 401 and 402 eV are attributed to positively charged imine (=NH^+) and amine (–NH_2^+) groups of polypyrrole, respectively [28]. In the case of Naf–Ppy and Naf–Ppy–Pt before reduction, satellite peak around 404 eV was appeared. Naf–Ppy, Naf–Ppy–Pt 0 0 2 before, and after reduction had the peaks of positively charged nitrogen as well as those of neutral nitrogen, indicating that positively charged pyrrolinum groups of polypyrrole were interacted with sulfonic groups of Nafion or negatively charged Pt precursors ($PtCl_6^-$ or $PtCl_4^-$) as shown in FT-IR spectra. After reducing Pt precursors into Pt(0), the ratio of N^+/N was decreased with the increase in the neutral groups. This finding elucidates that as a consequence of the reduction of some of negatively charged Pt precursors into Pt(0), the number of positively charged pyrrolinum groups of polypyrrole interacting with Pt precursors was decreased to meet the electroneutrality between the charged species in the composite membranes.

Pt(4f7/2 and 4f5/2) spectra were also measured to support above results by means of proving the reduction of Pt precursor into Pt(0) and mutual interaction between negatively charged Pt precursors and positively charged polypyrroles, as shown in Fig. 4(B). Typically, the location of two Pt(4f) peaks depends on the oxidation state of Pt; Pt(0) about 71 and 74 eV, Pt(II) about 72 and 76 eV, and Pt(IV) about 74 and 77 eV [29]. Before reducing Pt precursors in Naf–Ppy–Pt 0 0 2, two peaks of oxidized Pt(IV) were dominant, in spite of superposition of other peaks. On the other hand, after reducing Pt precursors in Naf–Ppy–Pt 0 0 2, two peaks of Pt(4f7/2 and 4f5/2) were shifted to lower binding energy or less oxidized state, suggesting that negatively charged Pt precursors (Pt(II) or Pt(IV)), which were interacted

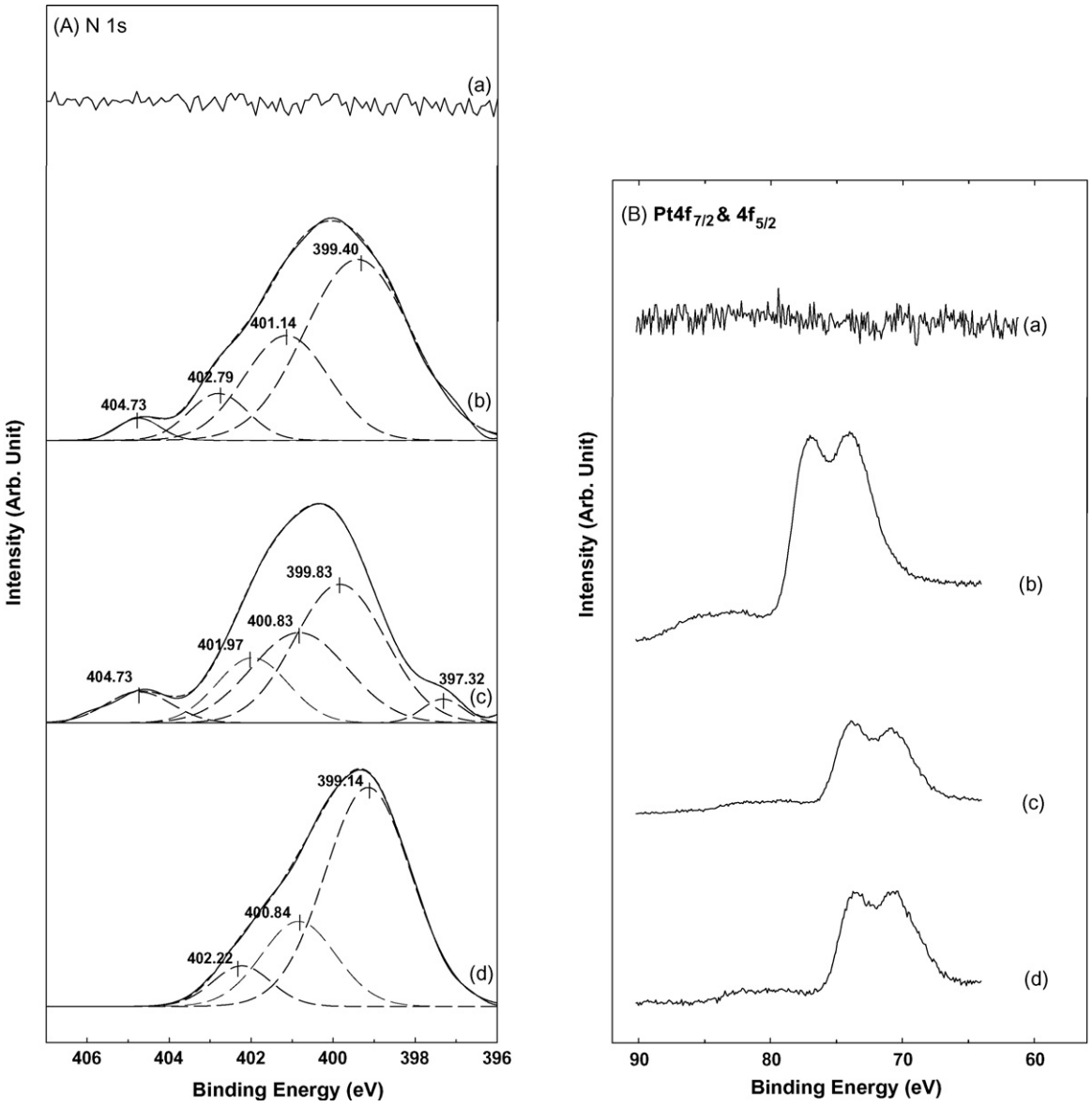

Fig. 4. (A) N 1s spectra of (a) Nafion, (b) Naf–Ppy, Naf–Ppy–Pt 0 0 2 (c) before and (d) after reduction; (B) Pt 4f7/2 and 4f5/2 spectra of (a) Naf-Pt, Naf–Ppy–Pt 0 0 2 (b) before and (c) after reduction, and (d) Naf–Ppy–Pt 0 0 4 after reduction; (C) O 1s spectra; (D) S 2p spectra of (a) Nafion, (b) Naf–Ppy, (c) Naf–Ppy–Pt 0 0 2, and (d) Naf–Ppy–Pt 0 0 4. All membranes were measured under dried condition.

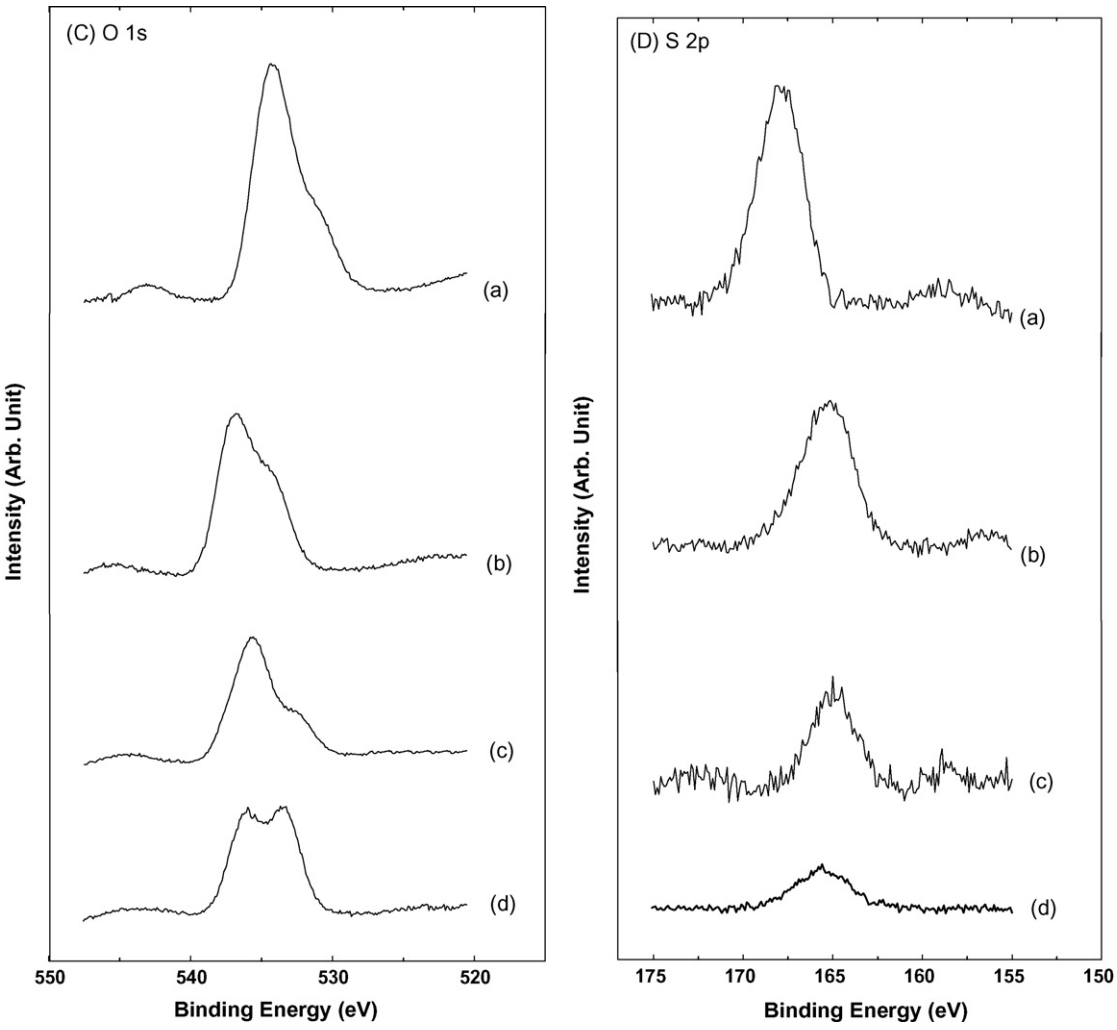

Fig. 4. (*Continued*).

with positively charged pyrrolinum groups of polypyrrole, were reduced to Pt(0). This peak shift in Naf–Ppy–Pt 0 0 2 before and after reduction was accompanied by the increment of neutral N–H groups. Considering the existence of broad peak even after the reduction, however, some of the oxidized Pt(II and/or IV) remained still in matrix. It is likely due to not oxidation but incomplete reduction of Pt ions into Pt(0) as a consequence of a fixation of Pt precursors on pyrrolinum groups of polypyrrole by means of electrostatic interaction. This finding was supported by the presence of small Cl peak after the reduction of Pt precursors. Comparing the peak area of Naf–Ppy–Pt 0 0 4 with that of Naf–Ppy–Pt 0 0 2, larger content of Pt of Naf–Ppy–Pt 0 0 4 compared to that of Naf–Ppy–Pt 0 0 2 was consistent with the result of quantitative analysis as shown in Fig. 2. When Pt precursors were introduced into Nafion matrix without pyrrole monomers, no peaks of Pt $4f_{7/2}$ or $4f_{5/2}$ were observed as shown in XPS spectra of Naf–Pt composite membrane. It was because negatively charged Pt precursors were excluded by Donnan effect attributed to electrostatic repulsion. When pyrrole monomers were diffused and polymerized at the surface of Nafion matrix, Pt precursors were also incorporated into Nafion matrix by means of electrostatic interaction with positively charged pyrrolinum groups. Therefore, positively charged pyrrolinum groups of polypyrrole played a role of assisting the co-incorporation of Pt precursors into Nafion matrix effectively by interacting with negatively charged sulfonic groups of Nafion and Pt precursors.

As shown in Figs. 4(C) and (D), O(1s) and S(2p) spectra of Nafion, Naf–Ppy, Naf–Ppy–Pt 0 0 2, and Naf–Ppy–Pt 0 0 4 reveal the relationship between pyrrolinum groups of polypyrrole and sulfonic groups of Nafion. In comparison to the peaks of O(1s) around 534 and 531 eV corresponding to ether groups and sulfonic groups of Nafion, respectively, those of composite membranes were shifted to higher binding energy as a result of introduction of polypyrrole into Nafion matrix. The presence of positively charged pyrrolinum groups of polpyrrole near the sulfonic groups led to the reduction of the electron density around oxygen atoms in Naf–Ppy and Naf–Ppy–Pt composite membranes relative to original Nafion [22,24,30,31]. This change in the O(1s) peak was compensated by the shift of S(2p) peak to lower binding energy [22,24,30,31]. Thus, electrostatic interaction between sulfonic groups of Nafion and pyrrolinum groups of polypyrrole altered chemical environment around sulfonic groups of Nafion. Furthermore, smaller portion of sulfonic O(1s)

than ether O(1s) in Nafion indicates that sulfonic groups were displaced preferentially towards the bulk away from the surface under drying condition [32]. Taking into consideration that peak of sulfonic O(1s) in composite membrane was more developed than that of Nafion, the reorientation of sulfonic groups towards surface occurred [32]. This morphological reorganization in the surface was strongly related to the incorporation of polypyrroles with Pt. The relative intensities of O(1s) and S(2p) of composite membranes compared to those of Nafion were weakened due to the presence of polypyrrole and Pt around the surface. In addition, considering the detection range of XPS, the evolution of sulfonic groups of Nafion after chemical in situ polymerization supported the presence of Ppy–Pt at the surface of matrix, as discussed in SEM and EPMA data.

3.3. Physical properties and cell performance of composite membrane for DMFC

Surface morphology of Nafion was influenced by the existence of polypyrrole and Pt. The physical and transport properties of Nafion for DMFC can be improved by the changes in the surface morphology after incorporating polypyrrole and Pt into composite system. Fig. 5 provides TGA curves and first derivative traces of Nafion, Naf–Ppy, Naf–Ppy–Pt 0 0 2, and Naf–Ppy–Pt 0 0 4. The Nafion membrane was decomposed into three stages: the desulfonation process at the first stage from 250 to 400 °C, the side-chain decomposition at the second stage from 400 to 500 °C, and PTFE backbone decomposition at the last stage from 500 to 600 °C [33]. In line with previous report [9], the peaks of the first stage in the first derivative curves of Naf–Ppy composites were shifted to a higher temperature due to the stabilization of the C–S bond with the formation of the Nafion–SO_3^- and $^+NH_2$–polypyrrole ionic pairs. The degradation of side chain in the second stage was also obstructed by mutual interaction. As the second peak was moved to higher temperature, two peaks of second and third stages could not be separated because of their superposition. Nearly complete superposition of second and third peaks of Naf–Ppy–Pt close to single peak, was associated with higher thermal stabilities of sulfonic groups and side chains of Naf–Ppy–Pt composites, compared to those of Naf–Ppy. In a similar manner to Naf–Ppy [9], Naf–Ppy–Pt composite membranes also had higher thermal stabilities of sulfonic groups and side chains than Nafion, resulting from electrostatic interaction between Nafion–SO_3^- and polypyrrole–NH_2^+ as described in XPS and FT-IR data. The composite membranes lost weight less than the pure Nafion up to ca. 500 °C, but the inversion of weight loss curves occurred above ca. 500 °C as shown in Fig. 5(A). This inversion may be lower stability of backbone attributed to the decrease in the crystallinity of the backbone as a result of the disruptive effect of side chain on the lamellar ordering of nonpolar backbone [34]. Nevertheless, the residual weights of Naf–Ppy–Pt composite membranes after the complete degradation of polymer backbone, were more than those of Nafion and Naf–Ppy due to the presence of thermally stable Pt.

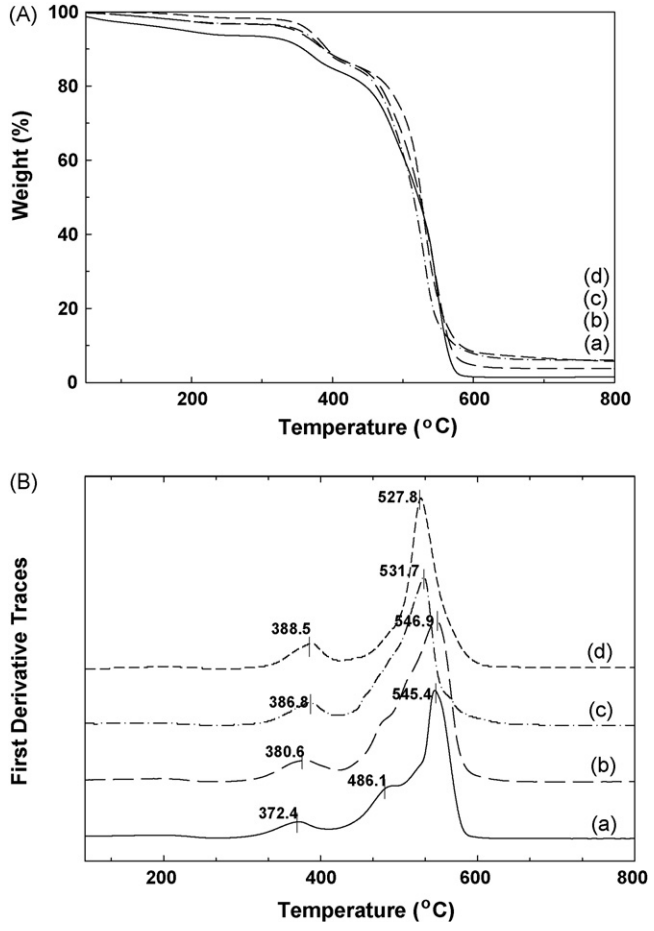

Fig. 5. (A) TGA curves and (B) first derivative traces of (a) Nafion (solid line), (b) Naf–Ppy (long dashed line), (c) Naf–Pt–Ppy 0 0 2 (5×10^{-3}) (dashed dot line), and (d) Naf–Pt–Ppy 0 0 4 (2×10^{-2}) (medium dashed line).

Transport properties of Nafion such as proton conductivity and methanol permeability as well as thermal stability should be improved to apply the composite membranes to a solid electrolyte. In particular, it is very important to reduce methanol crossover without decreasing proton conductivity for high performance in DMFC, because two kinds of transport properties are mainly accomplished by one transport pathway or ionic clusters. In this experiment, every transport result was averaged in the error range of ±7%. In order to clarify the effect of Pt content on the transport properties, proton conductivities and methanol permeabilities of composite membranes relative to those of Nafion were measured by changing Pt concentration from 10^{-4} to 2×10^{-2} M with a constant pyrrole concentration of 0.1 M, as shown in Fig. 6. As the concentration of Pt precursors increased, relative methanol permeability was decreased from 47.5 to 18.1% and relative proton conductivity was reduced from 78.6 to 69.2%. Both curves were linearly decreased along the *X*-axis of log scale. The slope of relative methanol permeability was sharper than that of relative proton conductivity in this measurement range. Typically, cell performance is proportional to proton conductivity and inversely proportional to methanol crossover, thereby suggesting that as the value of σ/P (σ is proton conductivity and P is methanol permeability) is enhanced, cell performance is improved. Taking into consideration that σ/P of Naf–Ppy–Pt 0 0 2 with the highest cell

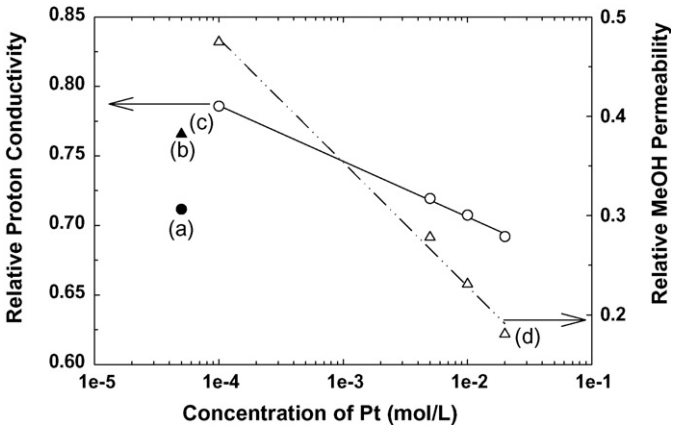

Fig. 6. (a) Relative proton conductivity (black circle) and (b) relative methanol permeability (black triangle) of Naf–Ppy. (c) Relative proton conductivity (white circle) and (d) relative methanol permeability (white triangle) of Naf–Ppy–Pt as a function of H_2PtCl_6 concentration at pyrrole concentration of 0.1 M.

performance among Naf–Ppy–Pt series was 2.59, while that of Naf–Ppy is 1.86, the co-introduction of Pt with polypyrrole ameliorated more favorably transport properties as well as thermal stabilities of Nafion. Fig. 7 shows polarization curves of Nafion and Naf–Ppy–Pt 0 0 2 in DMFC operation. We chose Naf–Ppy–Pt 0 0 2 among Naf–Ppy–Pt series and compared its performance with that of Nafion. Although proton conductivity of Naf–Ppy–Pt 0 0 2 was lower than that of Nafion or 71.9% relatively, the former had higher performance than the latter due to the decreased methanol crossover or 27.8% relatively. In the case of OCV related to methanol crossover, Naf–Ppy–Pt 0 0 2 had higher OCV values than Nafion at both 303 and 343 K due to its low methanol permeability. When operational temperature increased from 303 to 343 K and concentration of methanol from 3 to 6 M, the differences between cell performances of Nafion and Naf–Ppy–Pt 0 0 2 were larger. As the activity coefficient of methanol increased with its vaporization at 343 K and in more concentrated solution, methanol crossover rather than proton conductivity influenced total cell performance more strongly

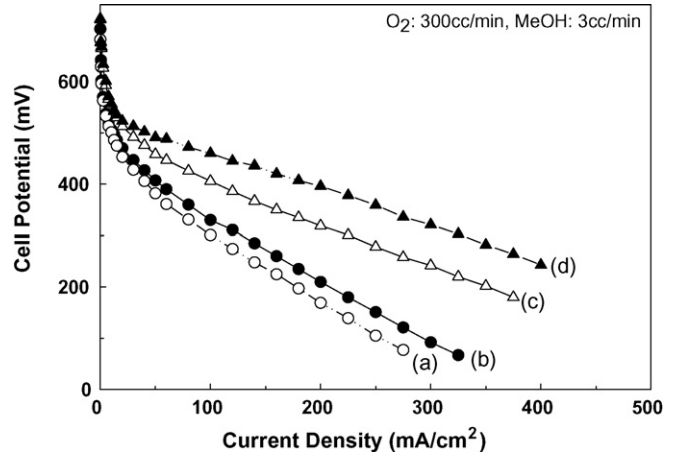

Fig. 7. *I–V* curves of (a) Nafion at 303 K under 3 M MeOH (while circle), (b) Naf–Ppy–Pt 0 0 2 at 303 K under 3 M MeOH (black circle), (c) Nafion at 343 K under 6 M MeOH (white triangle), and (d) Naf–Ppy–Pt 0 0 2 at 343 K under 6 M MeOH (black triangle).

[35,36]. Therefore, cell performance of Nafion was improved by the reduction of methanol crossover after incorporation and chemical in situ polymerization of pyrrole monomers with Pt.

4. Conclusion

Naf–Ppy–Pt composite membranes were fabricated by chemical in situ polymerization of pyrrole monomers with Pt precursors in Nafion matrix. The presences of polypyrrole and Pt around the surface region of composite membranes were proved by SEM and EPMA data. Positively charged pyrrolinum groups of polypyrrole were electrostatically interacted with sulfonic groups of Nafion as verified by XPS and FT-IR results, thereby assisting the incorporation of Pt into matrix. In addition, mutual interaction between Nafion–SO_3^- (or negatively charged Pt precursors) and polypyrrole–NH_2^+ influenced morphology as well as physical properties of pristine Nafion. Thermal property, proton conductivity, methanol permeability, and cell performance of pristine and modified Nafion were analyzed for an application of DMFC membrane. Thermal stabilities of sulfonic groups and side chains in Naf–Ppy–Pt composite membranes were higher than those of Nafion and Naf–Ppy, due to electrostatic interaction between sulfonic groups of Nafion and pyrrolinum groups of polypyrrole as well as the existence of thermally stable Pt. As the content of Pt was increased, methanol permeabilities of Naf–Ppy–Pt composite membranes were decreased from 47.5 to 18.1%, while their proton conductivities were reduced from 78.6 to 69.2% relative to those of Nafion. As a result of that, the enhancement of cell performance by Naf–Ppy–Pt 0 0 2 relative to Nafion was more pronounced under the specific experimental condition such as high temperature and more concentrated methanol solution where methanol crossover influenced overall performance dominantly.

Acknowledgements

This research was supported by New & Renewable Energy Project (Ministry of Commerce, Industry, and Energy). We thank them for funding.

References

[1] R.Z. Jiang, D. Chu, Solid State Lett. 5 (2002) A156–A159.
[2] R. Savinell, E. Yeager, D. Tryk, U. Landau, J. Wainright, D. Weng, K. Lux, M. Litt, C. Rogers, J. Electrochem. Soc. 141 (1994) L46–L48.
[3] M.V. Verbrudge, J. Electrochem. Soc. 136 (1989) 417–423.
[4] K.A. Mauritz, R.B. Moore, Chem. Rev. 104 (2004) 4535–4586.
[5] R. Basnayake, G.R. Peterson, D.J. Casadonte, C. Korzeniewski, J. Phys. Chem. B 110 (2006) 23938–23943.
[6] C. Heitner-Wirguin, J. Membr. Sci. 120 (1996) 1–33.
[7] E.B. Easton, B.L. Langsdorf, J.A. Hughes, J. Sultan, Z. Qi, A. Kaufman, P.G. Pickup, J. Electrochem. Soc. 150 (2003) C735–C739.
[8] B.L. Langsdorf, B.J. Maclean, J.E. Halfyard, J.A. Hughes, P.G. Pickup, J. Phys. Chem. B 107 (2003) 2480–2484.
[9] H.S. Park, Y.J. Kim, W.H. Hong, H.K. Lee, J. Membr. Sci. 272 (2006) 28–36.
[10] K. Bouzek, P. Holzhauser, R. Kodym, S. Moravcova, M. Paidar, J. Appl. Electrochem. 37 (2007) 137–145.
[11] S. Moravcova, K. Bouzek, Z. Cilova, J. Appl. Electrochem. 35 (2005) 991–997.

[12] F.F. Fan, A.J. Bard, J. Electrochem. Soc. 133 (1986) 301–304.
[13] G. Nagasubramanian, S. Dstefano, J. Moacanin, J. Phys. Chem. 90 (1986) 4447–4451.
[14] H. Yoneyama, T. Hirai, S. Kuwabata, O. Ikeda, Chem. Lett. (1986) 1243–1246.
[15] J.S. Do, W.B. Chang, Sens. Actuators B 101 (2004) 97–106.
[16] H. Nakano, Y. Tachibana, S. Kuwabata, Electrochim. Acta 50 (2004) 749–754.
[17] J.H. Park, J.H. Kim, H.K. Lee, T.H. Lee, Y.I. Joe, Electrochim. Acta 50 (2004) 769–775.
[18] H.Y. Lee, J.Y. Kim, J.H. Park, Y.G. Joe, T.H. Lee, J. Power Sources 131 (2004) 188–193.
[19] Y.J. Kim, W.C. Choi, S.I. Woo, W.H. Hong, J. Membr. Sci. 238 (2004) 213–222.
[20] V. Tricoli, J. Electrochem. Soc. 145 (1998) 3798–3801.
[21] Y.J. Kim, W.C. Choi, S.I. Woo, W.H. Hong, Electrochim. Acta 49 (2004) 3227–3234.
[22] S. Tan, A. Laforgue, D. Bélanger, Langmuir 19 (2003) 744–751.
[23] S. Tan, J.H. Tieu, D. Bélanger, J. Phys. Chem. B 109 (2005) 14085–14092.
[24] S. Tan, D. Bélanger, J. Phys. Chem. B 109 (2005) 23480–23490.
[25] H.S. Park, Y.J. Kim, W.H. Hong, Y.S. Choi, H.K. Lee, Macromolecules 38 (2005) 2289–2295.
[26] W. Kujawski, Q.T. Nguyen, J. Néel, J. Appl. Polym. Sci. 44 (1992) 951–958.
[27] A. Bernson, J. Lindgren, Solid State Ionics 60 (1993) 37–41.
[28] M.M. Chehimi, E. Abdeljalil, Synth. Met. 145 (2004) 15–22.
[29] C. Huang, K.S. Tan, J. Lim, K.L. Tan, Chem. Phys. Lett. 371 (2003) 80–85.
[30] S.H. Goh, S.Y. Lee, X. Zhou, K.L. Tan, Macromolecules 31 (1998) 4260–4264.
[31] X.L. Wei, M. Fahlman, K.J. Epstein, Macromolecules 32 (1999) 3114–3117.
[32] D. Susac, M. Kono, K.C. Wong, K.A.R. Mitchell, Appl. Surf. Sci. 174 (2001) 43–50.
[33] S.H. Almeida, Y. Kawano, J. Therm. Anal. Calor. 58 (1999) 569–577.
[34] B.R. Moore III, C.R. Martin, Macromolecules 22 (1989) 3594–3599.
[35] M. Hogarth, P. Christensen, A. Hamnett, A. Shukla, J. Power Sources 69 (1997) 113–124.
[36] M. Hogarth, P. Christensen, A. Hamnett, A. Shukla, J. Power Sources 69 (1997) 125–136.